THE FIAT LUX JOURNAL

2024

Volume I
Issue I

Table of Contents

The Fiat Lux Journal

The Variation of Renewable Energy in the Context of Global Economic and Social Well-Being

Raymond Wei[1]

[1]Crescent School

January 26, 2024

Abstract

As renewable energy (RE) rapidly integrates into society to meet the growing demand for affordable and clean energy (SDG 7, United Nations' Sustainable Development Goal 7), it is crucial to analyze the merits and flaws of renewable energy generation by assessing its impact on the global economy and social wellbeing. This paper performs an investigative study on the correlation and causality between renewable energy, economy, and environmental indicators. The data was gathered from diverse sources, including The Center for Climate and Energy Solutions, National Aeronautics and Space Administration Goddard Institute for Space Studies (NASA GISS), and Our World in Data, for the temperature, carbon dioxide (CO2) emissions, and gross domestic product (GDP) data. Significant Granger p-values were obtained for RE generation's ability to forecast CO2 emissions and temperature while discovering a strong positive correlation between CO2 and RE generation. The findings revealed that RE has limited effects on the global economy but has considerable implications on social and ecological wellbeing.

Keywords Renewable energy, CO_2 emissions, Average global real GDP per capita, Temperature, COVID-19 Pandemic

1 Introduction

As the global population rapidly approaches the carrying capacity of the logistic growth curve [1], the need for reliable energy sources becomes an urgent concern. According to the Klass Model [2], fossil fuel reserves for oil, coal, and gas are projected to deplete in approximately 35, 107, and 37 years, respectively. On the contrary, RE is inherently diversified, abundant, and mostly sustainable [3]. Therefore, the study of RE is crucial in ensuring the longevity of reliable energy sources for the future. On that account, it is critical for the scientific community to investigate the economic and environmental aspects of affordable and clean energy in pursuit of a sustainable future, which is the main purpose of the United Nations' Sustainable Development Goal 7: to ensure access to affordable, reliable, sustainable and modern energy for all [4]. The consistent performance of RE sectors before and during the Pandemic could attest to the degree of its resiliency during volatile times. Hence, the objective of this study is to analyze the relationship between RE, climate, and economic indicators before and amid the Pandemic. Discovering potential correlations between these variables will lead to a better understanding of the implications and feasibility of RE sources as it would inevitably become an integral component to the operation of future society. In our research, we have focused on the global data surrounding the generation of RE and its connection to CO_2 emissions, GDP, and global temperature.

2 Materials & Methods

2.1 Data

The global air temperature gridded data from the *NASA GISS Surface Temperature Analysis* [5] The dataset has a spatial resolution of 2x2 from 1980 to 2021. Data used in this table are from *Our World in Data*. Data includes the GDP per capita, PPP (constant 2017 international dollar), the global mean temperature anomalies (degrees Celsius), CO_2 emissions per capita (Tons), the energy produced by all the renewable sources (TWh), consisting of Wind, Solar, Hydro, Geo, Biomass, Waste, Wave, and

Year/World information)	GDP per capita, PPP (constant 2017 international $)	Global Mean Temperature Anomalies/degC	Co2 per capita tons	Wind - TWh	Solar - TWh	Geo, Biomass and Others - TWh	Hydro - TWh	Sum of all the renewables sources - TWh
2000	11079.91	0.39	4.11	31.42	1.32	181.97	2011.90	2870.48
2001	11196.19	0.54	4.09	38.39	1.49	190.80	2183.89	2823.48
2002	11350.08	0.63	4.13	52.33	1.78	208.29	2031.83	2892.23
2003	11827.33	0.62	4.29	82.91	2.28	217.83	2027.80	2950.83
2004	12085.46	0.54	4.45	85.12	2.97	225.21	2820.75	3144.04
2005	12301.04	0.68	4.55	104.08	4.88	234.51	2916.44	3279.19
2006	12941.19	0.64	4.62	132.88	5.72	271.83	3027.66	3437.88
2007	13193.27	0.67	4.70	170.88	7.78	294.85	3079.24	3552.55
2008	12835.75	0.54	4.72	220.60	12.61	313.31	3217.39	3803.91
2009	12581.81	0.66	4.60	276.62	20.84	328.82	3252.00	3988.28
2010	13090.11	0.72	4.79	348.47	23.87	383.03	3521.17	4300.99
2011	14260.38	0.61	4.90	440.39	40.38	402.01	3505.09	4469.30
2012	14339.90	0.65	4.91	510.53	101.16	438.16	3699.81	4717.89
2013	14883.14	0.68	4.89	631.99	138.94	474.37	3795.93	5041.92
2014	15177.20	0.75	4.87	705.81	197.76	510.48	3894.24	5308.29
2015	15510.60	0.90	4.81	831.43	256.36	548.64	3885.01	5519.44
2016	15828.68	1.02	4.75	982.23	328.29	580.88	4018.67	5909.97
2017	16242.88	0.92	4.76	1146.31	448.05	593.79	4066.72	6246.87
2018	16634.83	0.85	4.80	1269.52	578.91	632.17	4178.69	6653.33
2019	16911.29	0.98	4.76	1418.17	707.82	683.13	4227.88	7037.31
2020	16194.04	1.02	4.47	1591.28	855.72	700.07	4296.80	7443.81

Table 1: Data used in research

Tidal.

2.2 Tools

In this paper, Python version 3.8 is utilized for data analysis and visualization. Several Python modules such as NumPy, Pandas, Matplotlib, and sci-kit-learn are applied to plot the maps and the estimate of linear correlation. The time series were plotted using R version 4.1.2. The Pearson linear correlation is applied to estimate the relationship between RE use and other factors, including global mean surface temperature, CO_2 emissions, and GDP during the past decades. The Granger causality test is also used to determine causality between each variable.

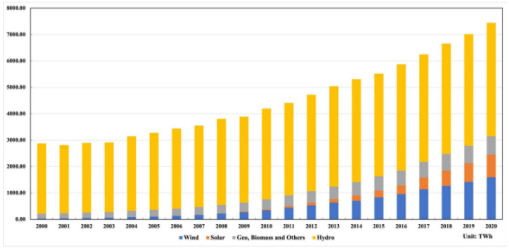

Figure 1: Contributions of wind, solar, hydro, geo, biomass, waste, wave and tidal.

2.3 Reducing Bias

The variables that we analyze are reputable social, ecological, and economic welfare indicators over the past two decades. We chose total global RE generation (terawatt hours) each year to gain a holistic insight into the prevalence of RE by factoring out outliers from particular countries. We did not choose to analyze the efficiency or price of RE because these indicators are more susceptible to measurement errors given the diverse nature of RE. Figure 1 shows the contribution of each major RE source to the total RE (in terawatt-hours) from 2000-2020 used in our calculations. Average global real GDP per capita (in constant 2017 international dollars) is the standard we chose to gauge worldwide economic activity. Real GDP accounts for current-year domestic output at current prices, thus neglecting inflation (whose increase does not signal real economic growth). Due to extreme economic disparities, the total real GDP is divided by the total global population to adjust for outliers. Environmentally, CO_2 emissions account for the highest concentration of greenhouse gas released into the atmosphere [6], hence providing a reliable quantitative measure of greenhouse gas emissions from human activities (notably due to the burning of fossil fuels). We gathered data of mean global temperature (in degrees Celsius) worldwide plotted by dividing longitude and latitude for our surface temperature and CO_2 emissions correlation map, ensuring reliable data over a large sample of regions. Throughout the paper, the average real global GDP per capita will be referred to as GDP, and total global RE generation annually may be abbreviated as RE.

3 Results

3.1 Time Series for CO_2, GDP, and RE respectively

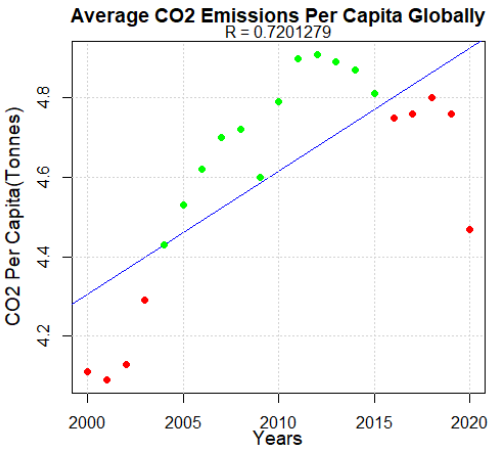

Figure 2: Average CO_2 emissions per capita globally in tonnes from 2000-2020 [7]. (Where red points represent the points below the expected values, and green points represent the points above the expected values)

The most significant deviations from the regression lines are in the years 2000-2003 and 2020. In the years 2000-2003, the deviation from the expected values was due to the exponential growth of CO_2 emissions largely attributed to the sudden rising demand for energy. In 2020, amid the COVID-19 outbreak, there was a decrease in the use of transportation and a decrease in economic activity, thereby decreasing CO_2 emissions [8].

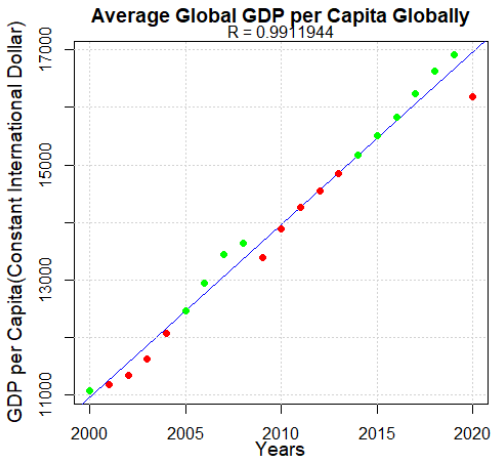

Figure 3: Average global GDP per capita from 2000-2020 [9].

The largest deviation in GDP per capita globally seems to be in 2020, which could mostly be explained by the decrease in economic activity due to the COVID-19 Pandemic.

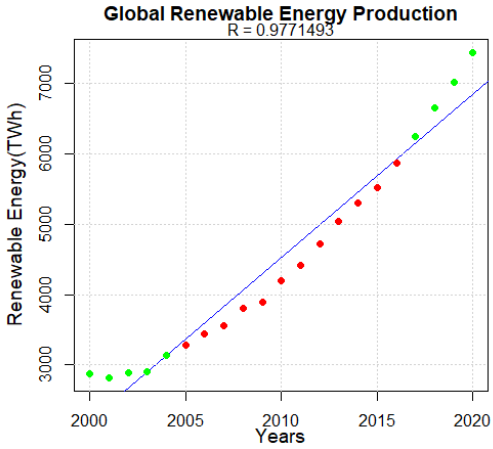

Figure 4: Global RE production in terawatt-hours from 2000-2020 [10].

There are no significant outliers in the data. However, despite the strong fit of the regression line, the data points seem to fit a growth curve whose increasing slope suggests that RE production worldwide has experienced accelerated growth over the past two decades.

3.2 Pearson Correlation

A correlation graph of RE, GDP, surface temperature, and CO_2 emissions suggests that these variables show a strong correlation and an upward trend. The data is normalized so that the standard deviations of each variable are compared for differences. Evidently, GDP and total RE are almost perfectly linear and correlated. Surface temperature and CO_2 emissions show

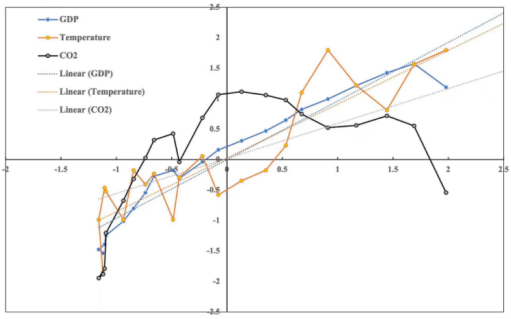

Figure 5: Standard deviations of CO_2 emissions per capita globally, average global GDP per capita, surface temperature (y-axis) with respect to standard deviation of global RE production (x-axis).

more substantial fluctuations but seem to also adhere to the general upward trend. Figure 5 depicts the standard deviation of RE (x-axis) with respect to CO_2 emissions, GDP, and temperature (y-axis). The data is normalized so that the variability of CO_2 emissions, GDP, and temperature can be compared to the variability of RE under a standard unit (the Z-score value). The least-squares regression lines are plotted for each variable. The sum of GDP residuals is significantly lower than that of CO_2 emissions and temperature. Therefore, the variability between RE and GDP is very similar, with few outliers whose presence could be attributed to external factors unrelated to RE that year.

3.3 Granger Causality Test

Using the Granger Significance test, we found no significant evidence that the explanatory variable (RE production) can predict the response variable (GDP per capita globally), where the p-value is 0.0849 is above the alpha level we chose of 0.05. Inversely, the GDP per capita globally cannot predict RE production, where the p-value is 0.256. However, we did find significant evidence that RE production can forecast CO_2 emissions per capita, where the p-value is 0.02372. The CO_2 emissions per capita cannot predict RE production, as we obtained a p-value of 0.1362. We found that RE production can forecast the global mean temperature, with a p-value of 0.0040238. Inversely, global mean temperature cannot predict RE production, as the test yielded a p-value of 0.091372.

3.4 Variable Anomalies

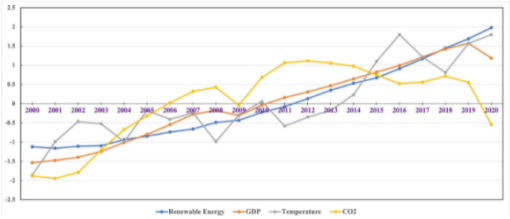

Figure 6: Graph of standard deviations of CO_2 emissions per capita globally, average global GDP per capita, surface temperature (y-axis) each year (x-axis).

There seems to be an "equilibrium relationship between green energy use, carbon emissions, and economic growth" [11]. Such a relationship can be shown in Figure 5. For example, economic growth, carbon emissions, temperature, and RE production all share a common upward trend. Also, the relationship between carbon emissions and green energy production shows that whenever the residual of one variable is negative, the residual of the other tends to be positive. In the years 2005 to 2015, the residuals for CO_2 emissions per capita globally were positive, shown by the green colour of the points, meanwhile, the residuals for RE generation globally were negative, shown by the red colour of the points. Both trends seem to occur at similar times, where the residuals for RE were negative from 2005 to 2016, while the residuals for CO_2 emissions were positive from 2004 to 2015.

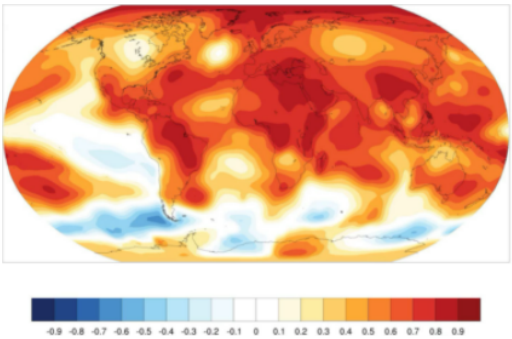

Figure 7: Correlation Map between Surface Temp. and CO_2 Emissions globally

4 Discussion

4.1 Connection Between RE, GDP and CO_2 Emissions

Rapid advancements in technology through the 21st century have significantly boosted economic growth through improved education, labour productivity, and ease of trade. Concurrently, the increasing worldwide population and CO_2 emissions of greenhouse gases have stimulated the growth of the RE sector [12]. Therefore, RE, GDP, and CO_2 have been overall trending upwards for the past two decades. However, Figure 5 depicts that GDP and CO_2 have experienced significant deviations from the steadily increasing trend since 2019. GDP has decreased to its 2017 levels while CO_2 emissions have fallen to 2010 levels. These outliers are primarily due to the effects of the COVID-19 Pandemic [13]. The Pandemic has disrupted trade, caused workplace absenteeism, and undermined job security worldwide [14]. Overall the economic implications of the Pandemic have been detrimental, which could explain why GDP has decreased since 2019 in Figure 3. CO_2 emissions have also declined sharply as manufactured products from fossil fuel combustion and cement production, accounting for roughly 29% of the global CO_2 emissions, has reduced significantly due to COVID-19 [15]. Evidently, the Pandemic has underscored the volatility of the fossil fuel industry. However, despite the economic downturn and weakening fossil fuels industry, RE production has demonstrated its resiliency by continuing its steady upward trend in production (shown in Figure 4). Extrapolating from these findings, perhaps RE could continue to display reliability as it integrates into society as an indispensable source of energy for the future.

4.2 Social Implications of Hydroelectricity

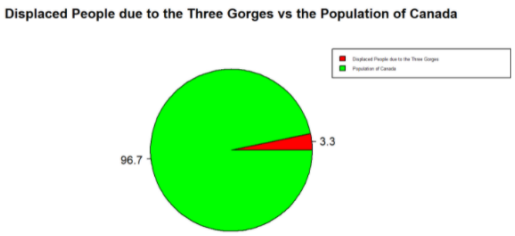

Figure 8: Pie chart showing the percentage of people displaced by flooding from the Three Gorges to the total population of Canada [16].

From Figure 1, it can be seen that hydroelectricity is by far the most used form of RE today, making up around 16% of the total global energy consumption [17]. However, the prevalence of hydroelectric dams has yielded negative social externalities. For example, the Three Gorges Dam in China, although is an indispensable energy source generating 88.2 billion kWh annually

[18], has become a major social concern. Along with the flooding of 13 cities, 140 towns, and 1350 villages, totaling 1.3 million residents being displaced [16]. Farmers and fishermen who lived near the Yangtze River (where the dam is located) were moved to cities, where they were structurally unemployed. As shown in Figure 8, the number of people displaced by the flooding of the Three Gorges Dam is equivalent to 3.3% of the entire population of Canada in 2021. Other hydroelectric dams worldwide also face similar problems. Therefore, the social implications of RE should be thoroughly considered before increasing generation capacity.

4.3 Socially Responsible RE Production

The Granger causality test proves that increased RE production could potentially be used to forecast rising temperatures, albeit the effect may be weak due to other confounding variables (such as greenhouse gas emissions, melting ice caps, etc.). Regardless, this result could potentially impose significant implications on how RE can be used in the future as a sustainable source of energy. Statistically, a p-value of 0.02372 supports that the RE generation trend could forecast CO_2 emission trends. In addition, the operation and creation of hydroelectricity present many environmental issues, one being the rise in temperature. Hydropower may seem sustainable when looking at its carbon footprint. However, water storage and hydroelectricity production emit millions of tons of methane, which has 86 times more warming power than CO_2. According to the *Environmental Defense Fund*, there are over 100 hydroelectric facilities in the world whose greenhouse gas emissions cause more significant warming than fossil fuel plants [19]. As a result, diversification in RE is crucial in ensuring its sustainability. Another form of RE that further adds to the global warming issue is biomass energy. Biomass energy is collected through the burning or decomposition of organic matter. Although biomass energy is renewable, it is not necessarily a sustainable energy source. According to *The Partnership for Policy Integrity*, biomass energy production emits 150% more CO_2 than coal energy production and 300 - 400% more than natural gas production [20]. Furthermore, biomass energy is usually a by-product of mass deforestation; therefore, the energy itself is indirectly non-renewable as its collection methods pose significant threats to the environment. Consequently, it can be seen that biomass energy production leaves a large carbon footprint and contributes to global warming as it

Linear Correlation	GDP		Temperature		CO2	
	Coefficient	R-square	Coefficient	R-square	Coefficient	R-square
Total Renewable Energy	0.96	0.93	0.89	0.78	0.53	0.33
Wind	0.93	0.87	0.9	0.79	0.44	0.23
Solar	0.83	0.67	0.87	0.70	0.23	0.08
Hydro	0.99	0.98	0.83	0.71	0.7	0.54
Geo, Biomass and Others	0.98	0.96	0.88	0.79	0.59	0.40

Table 2: Correlation Coefficients for each variable

emits significantly more CO_2 than many larger non-renewable energies. The positive correlation and significant casualty results between RE and temperature could imply potential issues with current RE generation (predominantly hydroelectric facilities). However, it is unlikely that the strong, positive correlation between RE production and CO_2 emissions is entirely a cause-and-effect relationship. On the contrary, the shape of the RE generation data points has displayed accelerated growth whose slope is increasing as time increases while the CO_2 emissions trend generally has a decreasing slope. It is very likely that the increased diversification of RE production in recent years (shown in Figure 1) has led to this result. Therefore, socially responsible production of RE should involve a variety of RE sources (such as solar, wind, etc.) so negative externalities can be mitigated.

4.4 Pearson Regression Analysis

Numerically, the linear correlation table shows that total RE production and GDP per capita share an R-squared value of 0.93. The linearity (stability) of GDP per capita is partially attributed to the large sample size as the real GDP per capita is average across the globe so singular outliers would not have significant impacts on the mean. Namely, the GDP per capita in 2008 had a Z-score of -0.5 despite the Great Recession in the U.S. (the world's leading power) that year. On the other hand, total RE and surface temperature share a relatively weaker correlation, although they still appear to be strongly correlated with an R-squared value of 0.78. This relationship aligns with a previous study, *The Economics of Renewable Energy*, stating that "if the worst impacts of rising temperatures and climate alteration are to be avoided, society needs to switch to renewable energy sources" [21]. Thus, they imply that rising temperature is closely correlated with insufficient RE usage, lining up with our results. We hypothesized that CO_2 emissions and RE would yield a negative correlation such that increased RE is accompanied by decreased CO_2 emissions as RE would replace the carbon-emitting fossil fuels. However, our results suggest a weak correlation between these two variables, where the R-squared value is 0.33. This result can imply that RE in the short-run (20 years) is not a perfect substitute for fossil fuels, or there may be other confounding vari-

ables (not analyzed by this paper) affecting CO_2 emissions, thus contributing to the weak correlation. We speculate that the increase in RE simply satisfies the continuously increasing demand for energy sources rather than substitutes for existing non-RE sources such as fossil fuels.

4.5 Potential Sources of Error

Given the limited scope of our research, there would inevitably be other variables not taken into account that may contribute to confounding errors. For example, the world's ecosystem and economy contain countless more intertwining variables than those explored in this paper. Therefore, relationships discovered through this paper are not solely dependent on the variables in the study, but may also be affected by other confounding variables. We encourage further experimental studies to validate and expand upon our results.

4.6 Summary and Conclusion

The implications of increased future RE production are clouded with uncertainty. This paper investigates how RE production impacts society economically and socially. Variable anomalies, using normalized data for each indicator, suggest that increased RE production correlates positively with GDP, CO_2 emissions, and temperature. Upon performing the Granger causality test on the time series for each variable, we obtained significant p-values(below 0.05) for RE generation's ability to forecast only CO_2 emissions and temperature, but not for GDP. Evidently, these findings suggest that there are limited global economic implications for RE generation(according to variations in GDP). Interestingly, RE generation's impact on CO_2 emissions is ambivalent. The increasing generation of RE is correlated with the simultaneously increasing CO_2 emissions. However, it could also be interpreted that the decline of CO_2 emissions in recent years (or, during some years, its decelerating upward trend) could be attributed to marginally increasing RE generation (increasing at an increasing rate). We hypothesize that other confounding factors, such as the combustion of hydrocarbon fuels, cause CO_2 emissions to increase while increased RE production slows the upward trend, although we lack empirical evidence to make this conclusion. However, we can safely conclude that dependence upon undiversified RE production yields detrimental negative social externalities. For example, the prevalent use of hydropower has led to the loss of many lives and displaced many others due to flooding (which is also due to rising temperatures). In conclusion, the RE generation's economic, environmental, and social implications explored in this paper should be considered as the era of rapid RE generation is on the horizon. In addition, future research is required to understand the relationship between RE generation and CO_2 emissions (to resolve our ambivalent results), and the magnitude of RE generation's effect on CO_2 and temperature should be further investigated.

References

[1] Marchetti C, Meyer PS, Ausubel JH. Human Population Dynamics Revisited with the logistic model: How much can be modeled and predicted? [Internet]. Technological Forecasting and Social Change. North-Holland; Available from: https://www.sciencedirect.com/science/article/abs/pii/0040162596000017

[2] Shafiee S, Topal E. When will fossil fuel reserves be diminished? Energy policy. 2009 Jan 1;37(1):181-9.

[3] Rita E, Chizoo E, Cyril US. Sustaining COVID-19 pandemic lockdown era air pollution impact through utilization of more renewable energy resources. Heliyon. 2021 Jul 1;7(7):e07455.

[4] Goal 7 | Department of Economic and Social Affairs [Internet]. Department of Economic and Social Affairs: Sustainable Development. United Nations; Available from: https://sdgs.un.org/goals/goal7

[5] GISTEMP Surface Temperature Analysis: NOAA Physical Sciences Laboratory [Internet]. psl.noaa.gov. Available from: https://psl.noaa.gov/data/gridded/data.gistemp.html

[6] 15. Nordhaus WD. To Slow or Not to Slow: The Economics of The Greenhouse Effect. The Economic Journal. 1991 Jul;101(407):920.

[7] CO_2-Data/OWID–data.xlsx at master · Owid/-data · github [Internet]. owid–data. 2021. Available from: https://github.com/owid/-data/blob/master/owid–data.xlsx

[8] Kumar A, Singh P, Raizada P, Hussain CM. Impact of covid-19 on Greenhouse Gases Emissions: A critical review [Internet]. Science of The Total Environment. Elsevier; 2021. Available from: https://www.sciencedirect.com/science/article/pii/S0048969721054267

[9] -Data/OWID–data.xlsx at master · Owid/-data · github [Internet]. owid–data. 2021. Available

from: https://github.com/owid/-data/blob/master/owid–data.xlsx
[10] Renewable energy generation [Internet]. Our World in Data. Statistical Review of World Energy; Available from: https://ourworldindata.org/grapher/modern-renewable-energy-consumption?country= OWID_WRL
[11] Wang Y-li. Research on the relationship between green energy use, carbon emissions and economic growth in Henan Province [Internet]. Frontiers. Frontiers; Available from: https://www.frontiersin.org/articles/10.3389/fenrg.2021.701551/full
[12] Dong K, Hochman G, Zhang Y, Sun R, Li H, Liao H. emissions, economic and population growth, and renewable energy: Empirical evidence across regions [Internet]. Energy Economics. North-Holland; Available from: https://www.sciencedirect.com/science/article/pii/S0140988318303256
[13] Smith LV, Tarui N, Yamagata T. Assessing the impact of COVID-19 on global fossil fuel consumption and emissions [Internet]. Energy Economics. North-Holland; Available from: https://www.sciencedirect.com/science/article/pii/S014098832100075X
[14] Pak A, Adegboye OA, Adekunle AI, Rahman KM, McBryde ES, Eisen DP. Economic Consequences of the COVID-19 Outbreak: the Need for Epidemic Preparedness. Frontiers in Public Health [Internet]. 2020 May 29;8(241). Available from: https://www.frontiersin.org/articles/10.3389/fpubh.2020.00241/full
[15] Liu Z, Ciais P, Deng Z, Lei R, Davis S, Feng S, et al. Near-real-time data captured record decline in global emissions due to COVID-19 [Internet]. Available from: https://arxiv.org/ftp/arxiv/papers/2004/2004.13614.pdf
[16] Nunez C. Hydropower Facts and Information [Internet]. Environment. National Geographic; Available from: https://www.nationalgeographic.com/environment/article/hydropower
[17] Nordensvard FUand J. China dams the world: The environmental and social impacts of Chinese dams [Internet]. Available from: https://www.e-ir.info/2014/01/30/china-dams-the-world-the-environmental-and-social-impacts-of-chinese-dams/
[18] Three Gorges Dam Sets World Record on Annual Power Output [Internet]. en.sasac.gov.cn. Available from: http://en.sasac.gov.cn/2020/11/20/c_6065.htm#:~:text=With%20a%20total%20installed%20capacity
[19] Ocko I. Long considered a "clean" energy source, hydropower can actually be bad for climate [Internet]. Energy Exchange. Environmental Defense Fund; Available from: https://blogs.edf.org/energyexchange/2019/11/15/long-considered-a-clean-energy-source-hydropower-can-actually-be-bad-for-climate/
[20] Carbon emissions from burning biomass for energy [Internet]. Biomass Energy Overview (updated April 2011) - PFPI. The PFPI; Available from: https://www.pfpi.net/wp-content/uploads/2011/04/PFPI-Biomass-Overview-April-2011.pdf
[21] Timmons D, Harris JM, Roach B. The economics of renewable energy. Global Development And Environment Institute, Tufts University. 2014;52:1-52.

The Fiat Lux Journal 2024

DYNAMIC CONVOLUTIONAL NETWORKS FOR 3-DIMENSIONAL RECONSTRUCTION

Dongchen Han

Phillips Academy Andover

January 22, 2024

Abstract

Modern convolutional neural networks (CNNs) require applying duplicate and redundant operations (such as alignment and matching) on different regions and pixels when processing three-dimensional (3D) reconstruction tasks. But different image areas and pixels are certainly not equally valuable for 3D reconstruction. In order to solve this problem, we propose a dynamic CNN structure for 3D reconstruction, which can dynamically modify the network based on the estimated impact of different regions and pixels on the 3D reconstruction task. The small gating branch learns which important areas or pixels need to be evaluated. The discrete gating decisions are trained with the Gumbel-Softmax trick, combined with a series of spatial and scale criteria. Our experiments on ShapeNet dataset shows that our method has higher accuracy than existing methods due to the better focus on important regions. Moreover, with an efficient CUDA implementation, our method achieves an improved inference speed on the most famous 3D reconstruction model Mesh R-CNN.

Keywords 3D Reconstruction, Dynamic Convolutional Neural Network

1 Introduction

With the development of virtual reality and deep learning, 3D reconstruction technology has been widely studied. It is worth noting that more and more preliminary research works began to use convolutional neural networks (CNNs) to reconstruct 3D shapes based on input RGB images. Although some progress has been made, these methods have a common significant shortcoming. In these methods, the same and redundant matching and alignment operations are performed for all regions and pixels. Obviously, these violent matching and alignment operations are unreasonable for 3D reconstruction tasks for three reasons. First, performing the same operation on different regions and pixels makes the existing 3D reconstruction system unable to effectively use different 3D reconstruction granularities in different image regions according to the characteristics of the object. Second, uniform matching and alignment operations also increase parameter redundancy and limit the performance of existing 3D reconstruction models on different scenes and objects in the natural world. Finally, redundant parameters can also significantly increase the training and test time. To solve these problems, we adopt an improved 3D reconstruction sub-network with a dynamic residual module, which can be trained end-to-end without additional space and scale constraints. Compared with the conventional CNN that performs the same convolution operation on all regions and pixels, our dynamic CNN can perform more convolution operations on image regions and pixels with more details. We borrowed design ideas of dynamic convolution [1] and residual convolution networks [2]. A dynamic residual module consists of several dynamic residual blocks. In every block, a small gating unit is used to select the regions that need to be focused on. The gating units are designed with the Gumbel-Softmax [3] trick to enable end-to-end training. Those decisions progress can extract features from important regions in the image, which enables the network to utilize higher-level information and process the regions of interest (ROIs) only. In addition, to improve the execution efficiency of the existing 3D reconstruction model, we implement the dynamic 3D reconstruction sub-network based on the CUDA platform of NVIDIA graphics cards. The core advantage of our approach is that we reduce as many CUDA modifications as possi-

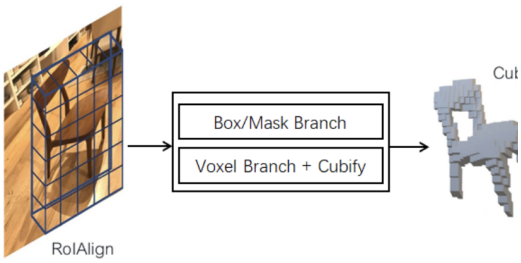

Figure 1: The overall structure of Mesh R-CNN. The voxel branch generates the coarse shape of each detected object. In the mesh refinement branch, several refinement stages can improve the details. We optimize the 3D reconstruction sub-network (i.e., mesh refinement branch) of Mesh R-CNN with the dynamic residual module.

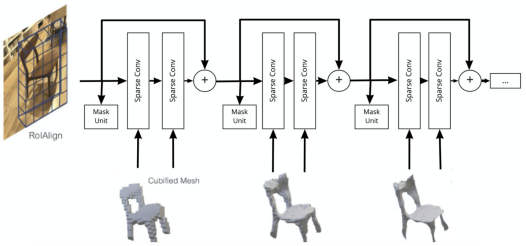

Figure 2: Our improved 3D reconstruction sub-network. Specifically, it adds multiple dynamic residual blocks to ROI Align to learn the target object's three-dimensional shape. Here we only list three dynamic residual blocks due to limited space. We use a mask unit and several spatial convolutions to learn the three-dimensional shape for each block.

ble. On the other hand, we optimized the Tensor data structure in memory. Compared to conventional CNNs, our method can perform convolution operations more accurately and sparsely. The main contributions of our paper are listed as follows: • We propose a dynamic 3D reconstruction sub-network to perform more precise and detailed convolution operations on image regions and pixels that need to be focused on in 3D reconstruction. We adopt the design idea of the Gumbel-Softmax trick to construct a dynamic residual module with gating masks. • The dynamic residual module can be integrated into existing 3D reconstruction networks based on convolutional layers. In the experiment, we combined our method into the most advanced Mesh R-CNN method. The results show that the proposed dynamic residual module can effectively improve the accuracy of Mesh R-CNN and accelerate the training and testing time of the entire network. • We implement the residual module on GPU with CUDA. It can not only theoretically reduce the number of floating-point operations but also practically accelerate the training and testing of Mesh R-CNN.

2 Methods

2.1 Tools

In this paper, we propose a dynamic 3D reconstruction sub-network based on dynamic residual modules, which can perform precise and detailed convolution in neural networks for 3D reconstruction. To show the effectiveness of the proposed method, we integrate it into the Mesh R-CNN system [26]. Figure 1 shows the system overview of Mesh R-CNN, where a 3D reconstruction sub-network is adopted in the mesh refinement branch. The original Mesh R-CNN has a common significant shortcoming, especially when facing redundant matching and alignment operations performed for all regions. The violent matching and alignment operations are inefficient in 3D reconstruction tasks. Performing redundant operations across different regions will be ineffective for applying different granularities on the final reconstructed object. This violent alignment operation will also increase parameter redundancy, causing difficulty processing other natural world scenes and increasing training time. To solve this problem, we optimize the 3D reconstruction sub-network of Mesh R-CNN with a dynamic residual module. With the dynamic processes in different regions, it can perform convolution operations with more details. In this section, we describe the design of the dynamic 3D reconstruction sub-network, which is based on dynamic residual modules.

2.2 Related Work

Our research aims to optimize the convolution operation in the existing 3D reconstruction model. Recently, more and more methods have begun to use CNNs for single-image 3D reconstruction. In general, these methods can be divided into three categories as follows. (1) Some approaches can predict the orientation of the shape [4, 5], and others can construct a 3D pose model based on the existing shape [6, 7, 8]; (2) Other methods predict 3D shapes based on point clouds [9, 10], patches [11, 12], or geometric primitives [13, 14, 15]; (3) Others use CNNs to learn distance functions [16]. Although these methods can perform 3D shape reconstruction well, they rely too much on data preprocessing and data post-processing steps, and these methods generally lack scalability. In addition, there

are some studies that mainly focus on multi-view reconstruction. Various methods are designed for it, including classical binocular stereo [17, 18], shape priors [19, 20, 21, 22], and modern learning techniques [23, 24, 25]. Our improved 3D reconstruction sub-network is shown in Figure 2. Specifically, our method adds multiple dynamic residual blocks to ROI Align to learn the target object's three-dimensional shape. Here we only list three dynamic residual blocks due to limited space. In each block, we use a mask unit and several spatial convolution layers to learn the three-dimensional shape. The spatial positions to be processed are indicated by the pixel-wise masks. For every dynamic residual block, we use the Gumbel-Softmax trick to enable the end-to-end training of discrete decisions, which can achieve better performance than REINFORCE [27] with less complexity. In the following, we will introduce in detail the dynamic residual block. Specifically, the structure of the dynamic residual block is shown in Figure 4. We denote the input of a block b (i.e., Cubified Mesh) as $X_b \in R^{c_b \times w_b \times h_b}$ and its output as $X_{b+1} \in R^{c_{b+1} \times w_{b+1} \times h_{b+1}}$. The dynamic residual block is formulated as:

$$X_{b+1} = r(F(X_b) + X_b)$$

where F is the dynamic function and r is the activation function. We make the values of F conditional on X_b by adopting a mask unit $M(X_b)$, which outputs soft gating decisions. Furthermore, we use the Gumbel-Softmax unit G to turn soft decisions $M_b \in R^{w_{b+1} \times h_{b+1}}$ into hard decisions $G_b \in R^{w_{b+1} \times h_{b+1}}$, indicating which position in the residual block should be evaluated. The Gumbel-Softmax unit can be described by:

$$G_b = G(M(X_b)).$$

Thus, the dynamic function F can be defined as:

$$F(X_b) = f(X_b) \circ G_b$$

where f is the spatial convolution function, which typically consists of two or three convolution layers with batch normalization (BN) [28]. The operation $\circ$ is the element-wise multiplication over the spatial dimensions broadcasted to all channels. Thus, a dynamic residual block can be represented by:

$$X_{b+1} = r(f(X_b) \circ G_b + X_b)$$

Figure 3 presents an example of the dynamic function F on a 6 × 5 × 1 feature map. The Gumbel-Softmax unit G selects the entries to be passed to the next dynamic residual block. The non-zero entries in $F(X_b)$ are significantly less than $F(X_b)$, which inspires us to accelerate the computation utilizing the sparsity of dynamic residual blocks.

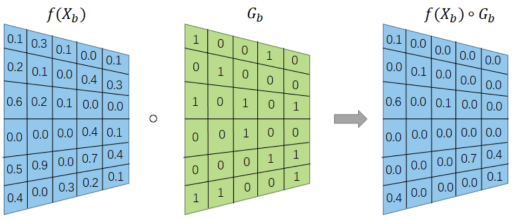

Figure 3: An example of the dynamic function $F(X_b) = f(X_b) \circ G_b$ The sparsity of $F(X_b$ is obviously higher than $F(X_b$, which can be utilized to reduce the amount of computation.

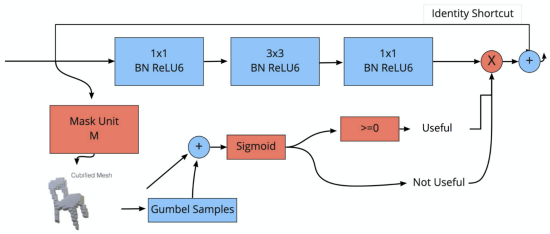

Figure 4: The execution flow of a mask unit with the Gumbel-Softmax trick. Firstly, a floating-point mask is generated. Then the soft decisions are converted into hard decisions by the Gumbel-Softmax trick, which enables the back-propagation for end-to-end learning.

2.3 Efficient inference implementation

Merely masking spatial locations in a convolutional block, as described above, does not lead to any speedup. During inference, our method needs evaluation on the active spatial positions only, indicated by Gb. Efficiently executing sparse operations is a challenging task. The overlap of convolutional kernels causes a single tensor element to be accessed several times, requiring advanced caching strategies. For instance, fast implementations of standard 3 × 3 convolutions use the Winograd algorithm [29], which processes image patches of typically 4 × 4 pixels. Conditionally executing individual pixels is not trivial in this case, and we leave the possibility to conditionally execute individual Winograd patches for future work. We propose a method to efficiently execute spatially sparse convolutions with minimal changes to existing operators. Our method executes individual operations conditionally by copying selected elements to an intermediate, dense tensor. For pointwise convolutions and activation functions, we can apply corresponding implementations on the intermediate tensor. Finally, the processed result is copied back to its original position.

3 Discussion

3.1 Dataset

ShapeNet [30] is a widely-used benchmark providing various 3D shapes, which are represented as textured CAD models and organized into semantic categories following WordNet [31]. We use a subset of ShapeNetCore.v1 to train and evaluate our method, like [26]. The meshes are rendered from at most 24 randomly chosen viewpoints. The RGB images are of size 137 × 137. The training and testing sets consist of 35,011 models (840,189 images) and 8,757 models (210,051 images), respectively. To evaluate the model, we input a single RGB image of a rendered ShapeNet model on a blank background and obtain the output, which is a 3D mesh of the object. The neural network is trained with pairs of images and meshes.

4 Discussion

4.1 Evaluation

We adopt evaluation metrics used in recent work [32, 33, 34, 26]. We compute Chamfer distance and $F1^{\tau}$ at various distance thresholds by sampling 10k points uniformly from the surface of predicted and ground-truth meshes. $F1^{\tau}$ is the harmonic mean of the precision and recall at *tau*. For Chamfer distance, lower is better. For $F1^{\tau}$, higher is better.

4.2 Analysis of Results

The results of our comparison with other state-of-the-art methods are shown in Table 1. For the sake of fairness, we comprehensively evaluated three evaluation measures. All the experimental results in the table are from the original paper. Because some methods do not share their source code, we cannot reproduce and make complete comparisons. In general, our method has achieved better results than other methods.

	Chamfer (↓)	$F1^{\tau}$ (↑)	$F1^{2\tau}$ (↑)
N3MR [35]	2.629	33.80	47.72
3D-R2N2 [36]	1.445	39.01	54.62
PSG [9]	0.593	48.58	69.78
Pixel2Mesh [34]	0.591	59.72	74.19
MVD [32]	-	66.39	-
GEOMetrics [33]	-	67.37	-
Mesh R-CNN [26]	**0.306**	**74.84**	**85.75**
Ours (Best)	**0.310**	**77.82**	**87.17**

Table 1: The comparison of single-image shape reconstruction on ShapeNet.

	Training time	Testing time
Mesh R-CNN	1.00	1.00
Ours (3 residuals)	0.82	0.93
Ours (4 residuals)	0.87	0.95
Ours (5 residuals)	0.92	0.97
Ours (6 residuals)	0.97	0.98

Table 2: The training and testing time of the original Mesh R-CNN and our method.

In careful comparison with the Mesh R-CNN method, our method has achieved better performance. In the experiment, the performance of our method will change with the number of dynamic residual blocks. Here we only list the best result of our method, which uses three dynamic residual blocks. In addition, we also compared the impact of our method on the training time and testing time of the original Mesh R-CNN method. The experimental results are shown in Table 2. Our method can optimize the testing and training time of Mesh R-CNN. Because of limited resources, we only test up to 6 residual modules. Our method achieves the best performance with three residual modules.

4.3 Examples of Reconstruction Results

We more intuitively compare our method and the original Mesh R-CNN on 3D reconstruction. We show part of the 3D reconstruction results in Figure 5. The last two columns of each result are the 3D triangle meshes generated by our method and Mesh R-CNN. From Figure 5, we can see that our method has achieved better results. Compared with the Mesh R-CNN method, our method can pay more attention to the detailed information in the 3D reconstruction details. Moreover, get a more accurate expression of the 3D triangle.

5 Conclusion

In our research project, we carefully survey the previous works on 3D construction. The state-of-the-art 3D construction models have similar problems: conventional CNNs can only operate the same convolution operations on all pixels of images and ignoring the detail of 3D shapes. Based on this observation, we propose a dynamic

Figure 5: We more intuitively compare our method and the original Mesh R-CNN on 3D reconstruction. The last two columns of each result are the 3D triangle meshes generated by our method and Mesh R-CNN.

3D reconstruction sub-network to improve the original frameworks of Mesh R-CNN. In the paper, we briefly illustrate our proposed method and analyze the experimental results. The proposed method outperforms Mesh R-CNN by a large margin with lower training and testing time.

References

[1] Thomas Verelst and Tinne Tuytelaars. Dynamic convolutions: Exploiting spatial sparsity for faster inference. In CVPR, pages 2317–2326, 2020.

[2] Kaiming He, Xiangyu Zhang, Shaoqing Ren, and Jian Sun. Deep residual learning for image recognition. In CVPR, 2016.

[3] Eric Jang, Shixiang Gu, and Ben Poole. Categorical Reparameterization with Gumbel-Softmax. 2016.

[4] David F. Fouhey, Abhinav Gupta, and Martial Hebert. Data-driven 3D primitives for single image understanding. In ICCV, 2013.

[5] Derek Hoiem, Alexei A. Efros, and Martial Hebert. Geometric context from a single image. In ICCV, 2005.

[6] Abhijit Kundu, Yin Li, and James M. Rehg. 3D-RCNN: Instance-level 3d object reconstruction via render-andcompare. In CVPR, 2018.

[7] Georgios Pavlakos, Xiaowei Zhou, Aaron Chan, Konstantinos G. Derpanis, and Kostas Daniilidis. 6-dof object pose from semantic keypoints. In ICRA, 2017.

[8] Shubham Tulsiani and Jitendra Malik. Viewpoints and keypoints. In CVPR, 2015.

[9] Haoqiang Fan, Hao Su, and Leonidas J. Guibas. A point set generation network for 3d object reconstruction from a single image. In CVPR, 2017.

[10] Chen-Hsuan Lin, Chen Kong, and Simon Lucey. Learning efficient point cloud generation for dense 3d object reconstruction. In AAAI, 2018.

[11] Thibault Groueix, Matthew Fisher, Vladimir G Kim, Bryan C Russell, and Mathieu Aubry. A papier-mâché approach to learning 3d surface generation. In CVPR, 2018.

[12] Peng-Shuai Wang, Chun-Yu Sun, Yang Liu, and Xin Tong. Adaptive O-CNN: a patch-based deep representation of 3d shapes. In SIGGRAPH Asia, 2018.

[13] Sanja Fidler, Sven Dickinson, and Raquel Urtasun. 3d object detection and viewpoint estimation with a deformable 3d cuboid model. In NeurIPS, 2012.

[14] Yonglong Tian, Andrew Luo, Xingyuan Sun, Kevin Ellis, William T. Freeman, Joshua B. Tenenbaum, and Jiajun Wu. Learning to infer and execute 3d shape programs. In ICLR, 2019.

[15] Shubham Tulsiani, Hao Su, Leonidas J. Guibas, Alexei A. Efros, and Jitendra Malik. Learning shape abstractions by assembling volumetric primitives. In CVPR, 2017.

[16] Lars Mescheder, Michael Oechsle, Michael Niemeyer, Sebastian Nowozin, and Andreas Geiger. Occupancy networks: Learning 3d reconstruction in function space. In CVPR, 2019.

[17] Richard Hartley and Andrew Zisserman. Multiple view geometry in computer vision. Cambridge university press, 2003.

[18] Daniel Scharstein and Richard Szeliski. A taxonomy and evaluation of dense two-frame stereo correspondence algorithms. IJCV, 2002.

[19] Sid Yingze Bao, Manmohan Chandraker, Yuanqing Lin, and Silvio Savarese. Dense object reconstruction with semantic priors. In CVPR, 2013.

[20] Volker Blanz and Thomas Vetter. A morphable model for the synthesis of 3d faces. In SIGGRAPH, 1999.

[21] Amaury Dame, Victor A. Prisacariu, Carl Y. Ren, and Ian Reid. Dense reconstruction using 3d object shape priors. In CVPR, 2013. [22] Christian Häne, Nikolay Savinov, and Marc Pollefeys. Class specific 3d object shape priors using surface normals. In CVPR, 2014.

[23] Abhishek Kar, Christian Häne, and Jitendra Malik. Learning a multi-view stereo machine. In NeurIPS, 2017.

[24] Alex Kendall, Hayk Martirosyan, Saumitro Dasgupta, Peter Henry, Ryan Kennedy, Abraham Bachrach, and Adam Bry. End-to-end learning of geometry and context for deep stereo regression. In ICCV, 2017.

[25] Tanner Schmidt, Richard Newcombe, and Dieter Fox. Self-supervised visual descriptor learning for dense correspondence. In IEEE Robotics and Automation Letters, 2017.

[26] Georgia Gkioxari, Jitendra Malik, and Justin Johnson. Mesh R-CNN. In ICCV, 2019.

[27] Ronald J Williams. Simple statistical gradient-following algorithms for connectionist reinforcement learning. Machine learning, 8(3-4):229–256, 1992.

[28] Sergey Ioffe and Christian Szegedy. Batch normalization: Accelerating deep network training by reducing internal covariate shift.

2015.
[29] Andrew Lavin and Scott Gray. Fast algorithms for convolutional neural networks. In CVPR, pages 4013–4021, 2016.
[30] Angel X. Chang, Thomas A. Funkhouser, Leonidas J. Guibas, Pat Hanrahan, Qi-Xing Huang, Zimo Li, Silvio Savarese, Manolis Savva, Shuran Song, Hao Su, Jianxiong Xiao, Li Yi, and Fisher Yu. Shapenet: An informationrich 3d model repository. In CoRR 1512.03012, 2015.
[31] George A. Miller. WordNet: A Lexical Database for English. In Commun. ACM, 1995.
[32] Edward Smith, Scott Fujimoto, and David Meger. Multi-view silhouette and depth decomposition for high resolution 3d object representation. In NeurIPS, 2018.
[33] Edward J. Smith, Scott Fujimoto, Adriana Romero, and David Meger. GEOMetrics: Exploiting geometric structure for graph-encoded objects. In ICML, 2019.
[34] Nanyang Wang, Yinda Zhang, Zhuwen Li, Yanwei Fu, Wei Liu, and Yu-Gang Jiang. Pixel2Mesh: Generating 3D mesh models from single RGB images. In ECCV, 2018.
[35] Hiroharu Kato, Yoshitaka Ushiku, and Tatsuya Harada. Neural 3D mesh renderer. In CVPR, 2018.
[36] Christopher B. Choy, Danfei Xu, JunYoung Gwak, Kevin Chen, and Silvio Savarese. 3D-R2N2: A unified approach for single and multi-view 3d object reconstruction. In ECCV, 2016.

Evaluation of Inconsistent Judgement Criteria in Ad Hoc Tribunals

Edmund Carr, Miles Boyer

January 25, 2024

Abstract

Evidence, in the form of facts and materials, is crucial in proving the truth of a matter in court. Oral testimonies, which are verbal statements made by witnesses during legal proceedings, serve as a key method of gathering evidence. In assessing these testimonies, judges closely examine both the content of the evidence and the witness's background to evaluate credibility and reliability. Reliability hinges on the testimony's quality and accuracy, while credibility is influenced by the witness's objectivity and competence. Objectivity is gauged by considering factors like bias, integrity, and demeanor. Competence, conversely, is determined by the witness's mental state, language proficiency, memory, and other elements that may affect their ability to provide reliable testimony. However, the delivery of evidence is prone to bias. For example, while objectivity aspects are to some degree in the conscious command of a witness, the issues of competence are mostly outside of the witness' control. As a result, evaluation of the evidence is made extremely difficult by the subjective and uncontrollable nature of oral testimonies. To prove the defendant's guilt "beyond reasonable doubt," judges must first presume innocence. This task becomes more complex when the primary evidence is derived from oral testimonies, where the judge's subjective perception may lie at the heart of the matter.

Keywords

Yugoslavia, Tribunal, Ad Hoc, ICTY

1 Introduction

According to the analysis of Chlevickaitė's article "Judicial Witness Assessments at the ICTY, ICTR, and ICC: Is There 'Standard Practice' in International Criminal Justice?", ICCT's legal frameworks do not offer guidelines for evidence assessment. As the precise parameters for credible and reliable testimonies are largely subjective, "confidence [is] vested in professional judges to bring sufficient experience to their jobs" (Chlevickaitė et al.). Judges in international crime tribunals face the complex task of traversing "cultural and linguistic barriers, time gaps, conflict-inspired biases, and traumatic circumstances" (Chlevickaitė et al.). This demands high flexibility, but the lack of concrete guidelines results in uncertainty and questions of fairness. Not only are judges "free to decide on the appropriate approach," (Chlevickaitė et al.) but the rules are also "open to interpretation and amendment" (Chlevickaitė et al.). The freedom delegated to judges stemming from the loose framework allows great room for error. Through the analysis of "all trial judgments issued by the ICTY, ICTR, and ICC," (Chlevickaitė et al.) justice practitioners were found to be susceptible to using alleged deception cues "without any reference to scientific knowledge or precedent" (Chlevickaitė et al.). Even in the case that judges do spot erroneous statements through inconsistencies in the witness's testimony, the freedom of discretion leaves a large margin for error. For example, in the case of assessing objectivity, the treatment of a witness' inconsistent behavior creates gray areas of little legal certainty; some judges may completely overlook inconsistencies that would be serious enough to destroy a witness's credibility. Other judges might see the inconsistencies as a mitigating factor to reduce the severity of the crime or choose to treat inconsistent evidence as exculpatory evidence and clear the defendant of wrongdoings. As a result of the inconsistent and shaky methodologies of assessing evidence, different judges may arrive at different or altogether incorrect conclusions.

2 Review of Objectivity and Competence Factors in Ad Hoc Tribunals

2.1 The Evolution of Judgement Standards

Chlevickaitė's article demonstrates that the guidelines for legal institutions, between 1995 and 2019, are experimental and constantly evolving. In the earliest judgment of the ICTY, the Tadić case, judges sought "minimal external guidance (domestic precedent and expert testimony)" (Chlevickaitė et al.) and the chamber "focused on responding to the challenges by the defense, which centered on witness objectivity." Essentially, the Tadić case gave judges the freedom to make judgments based on how the witness responds to the defense. On the other hand, the earliest ICTR judgment in the Akayesu case made "use of expert testimony," leading to "contribution to witness competence criteria." For example, by referring to factors such as trauma, PTSD, and time-lapse, judges had the discretion to "explain away" testimonial deficiencies. After 2004, the number of new indicators of reliability and credibility significantly reduced while "mostly insider-specific aspects are further developed." This period also saw a shift of focus from competence to objectivity indicators for assessing witness credibility. This change reflects a growing concern over the potential bias in witness testimonies as the emphasis is placed on "the assessment of insider, accomplice, or witnesses." Finally, the timeline demonstrates the reconciliation of cross-institutional inconsistency, especially after 2010. As the guidelines evolved, the existing judging criteria remained stable over time, with tribunals sharing many overlapping indicators in a process of cross-institutional learning.

2.2 Witness Memory

The witness's memory is a contentious issue in court as it pertains to the witness's competency. Historical records have proven that "it is nearly impossible to produce consistent accounts over time." Especially in the cases of traumatic events that the witness had experienced several years prior, any contradiction or gap in memory can weaken the testimony's credibility. Looking at Emil Čakalic's case against Slavko Dokmanović in 1998, Čakalic was especially susceptible to giving inconsistent accounts between his many written statements and multiple oral testimonies. The cross-examiner attempted to undermine Čakalic's case by identifying these contradictions in his recollections. The cross-examiner pointed out that while Čakalic testified to Dokmanovic beating Dado Dukic on November 19th, 1991 in Ovcara, Čakalic's supplementary statement reflected the opposite, which was that he did not actually "see who [Dokmanovic] was hitting" (ICTY Web) To put the witness's competence in further question, the defendant points out contradictions that pertain only to trivial details that do not affect the central components of the testimonies. For instance, the cross-examiner debated over the subtle differences in meaning between words such as "see" and "recognize" in questioning Čakalic. The cross-examiner stated that Čakalic "made a statement saying that [he] did not see other people [on the bus at Ovcara]" (ICTY Web) even though Čakalic testified he recognized people on the bus, to which Čakalic responded, "How could I say that I did not see anyone, there was a bus full of people" (ICTY Web). The case demonstrates that memory could expose vulnerabilities in their testimony as it is a key component of witness competency.

2.3 Witness Bias

The credibility of eyewitness testimony can also be undermined by the perceived bias of personally victimized individuals. For instance, the suffering experienced by victims may cause them to inadvertently "exaggerate the damage sustained" (Chlevickaitė et al.). This phenomenon was evident in the cross-examination of Nedeljko Draganić during his testimony against Zdravko Mucić, Hazim Delić, Esad Landžo, and Zejnil Delalić on April 2 and 3, 1997. The defense employed several strategies to prove Draganić's account was heavily exaggerated. The cross-examiner pointed out the witness's claim that "one [hit Cerici] every 40 seconds [which is] an outrageous amount of shells" (ICTY Web) The cross-examiner went on to further evoke doubt over Draganić's competency by questioning how he calculated the outrageous number despite his mathematics background. This exaggeration may have cast doubts on the other statements Draganićmade. As there was no evidence except verbal testimonies to support Draganić's claim that terrorists "beat [him] almost every day," (ICTY Web) Draganić could have overstated the number of beatings he has received. Thus, the credibility of the witness is crucially

important as any perceived exaggeration or bias in testimonies could impugn the overall truthfulness of the testimony.

2.4 Trauma and PTSD

Finally, trauma and PTSD may impact the reliability of a witness's statement. The foreign court environment, coupled with the stressful nature of recalling distressing events, can exacerbate anxiety and may "impair attention and memory processes" (Chlevickaitė et al.). This effect is particularly pronounced in vulnerable witnesses unfamiliar with Western court procedures, who may feel intimidated by the cross-examiner scrutinizing their testimonies and asking challenging questions. Looking back to the Čakalic case, the cross-examiner deliberately puts Čakalic in a stressful position by twisting his words (mixing up "see" and "recognize") and questioning his memory. Similarly, in Draganić's case, the defense strove "to manipulate the witness's emotional state to make [him] appear less credible" (Chlevickaitė et al.). The cross-examiner attempted to question Draganić's reliability by asking: "As an intelligent, educated man, are you saying you did not read the newspaper; you did not listen to the news?" (ICTY Web). The question serves to insinuate the witness's ignorance and incompetence to give accurate information. Lastly, Witness 87's case on April 2, 2000, further exemplifies this point. Witness 87, who had refrained from "discussing the abuses with anyone, including her mother," (ICTY Web) was pressured by the cross-examiner to divulge sensitive information. Upon receiving unsatisfactory answers, the cross-examiner complains that the witness "answered, 'I don't remember,' 49 times to my questions" (ICTY Web). These examples underscore the vulnerability exhibited by traumatized witnesses who may be indisposed to offer relevant and credible information.

3 Conclusion

From the study of the above three tribunal cases, it is evident that there is great potential for bias in both the narration of events by witnesses and the interpretation by judges. As historical events, when told through the lens of a witness, take the form of a biased story, courts should perform extensive background checks on the witness to understand how the narration of the story could be flawed. The courts would also benefit from the input of psychologists and psychiatrists to establish more consistent guidelines based on a more scientific approach. Finally, courts such as the ICC, should look to the jurisprudence established by other international tribunals instead of solely depending on their own precedences. Although relying on inside precedence may satisfy internal consistency, cross-institutional standards inevitably become divergent. Ultimately, the nature of tribunal judgments does not call for the standardization of all aspects. However, consistent guidelines informed by modern scientific understanding will facilitate more fair and transparent outcomes.

References

[1] Behrens, Paul. "Assessment of International Criminal Evidence: The Case of the Unpredictable Génocidaire." ZaöRV, vol. 71, 2011, pp. 661–689, www.zaoerv.de/71_2011/71_2011_4_a_661_690.pdf. Accessed 9 Dec. 2023.

[2] Chlevickaitė, Gabrielė. "Judicial Witness Assessments at the ICTY, ICTR, and ICC: Is There "Standard Practice" in International Criminal Justice?" Oup.com, 2023, academic.oup.com/jicj/article/18/1/185/5820566#204714342. Accessed 9 Dec. 2023.

[3] "Voice of the Victims | International Criminal Tribunal for the Former Yugoslavia." www.icty.org/en/features/voice-of-the-victims.

The Fiat Lux Journal

A Satellite Visual Analysis of the Albedo Effect on Glacial Recession, and its Use as a Predictor of Glacial Lake Changes

Jason Huang[1]

[1]Crescent School

January 26, 2024

Abstract

This paper reviews recent studies concerning the relationship between glacial recession over the past 100 years, the weakened albedo effect, and the glacial lake changes in the Hindu Kush Himalayan (HKH) region. Geological indicators provided by NASA Worldview's satellite images were used to verify an inverse correlation between the albedo effect and glacial recession. Confirmation of this inverse relation suggests changes in glacial lakes, which increases the risk of glacial lake outburst floods (GLOF) over time. This article also examines the impact of past GLOFs on the HKH region's population and assesses the vulnerability of local communities and infrastructure near potentially dangerous glacial lakes (PDGL). Understanding these relationships can ensure the safety of disaster-threatened communities and provide potential proactive measures that could prevent possible future lake outburst disasters.

Keywords Environmental Science, Ecosystem, Glacial Recession, Glacial Lake, Meltwater

1 Introduction

Since the early 1900s, glaciers worldwide have experienced rapid melting –with human innovation being the source of this phenomenon. Glacial recession is the process in which the ice ablates faster than snow can fall to accumulate and form new glacial ice. This process can be seen when the terminus, the glacier's snout or lowest end, does not extend as far down-valley as it did in previous times.' Studies have shown that Anthropogenic global warming has caused increases in Earth-surface temperatures, which significantly impacts the rate of glacial recession. In the Himalayan region, it is imperative to recognize and address these problems as many people rely on local lakes and rivers as their primary source of water. Over 2 billion people, roughly 20% of the world's population, depend on the Tibetan rivers for water and other resources. A large portion of this population (approximately 240 million people) reside in the Hindu Kush Himalayan region, which further extends the reasoning for sustaining this environment.2 In the HKH region (Figure 1), there are around 54,000 existing glaciers, consisting of clean and debris-covered ice, covering a total area of 60,000 km^2.' This cryospheric area, commonly referred to by the scientific community as the "Third Pole," has the highest concentration of snow and glaciers outside of Earth's poles. The HKH region is also built on one of the Earth's most dynamic river and mountain systems, enabling it to sustain complex hydrology and diverse environments. The ten central river systems include the Amu Darya, Brahmaputra, Ganges, Indus, Irrawaddy, Mekong, Salween, Tarim, Yangtze, and Yellow Rivers - all of which are fed by meltwater from the local glaciers.'The glaciers surrounding these rivers play vital roles in the availability of resources, the maintenance of the HKH region's diverse ecosystem, and the region's local infrastructure. Further glacial recession in the HKH region could profoundly impact the ecological equilibrium and present severe challenges to the communities that depend on them. An issue of acute concern regarding the glaciers in the HKH region, and more specifically the glaciers of the Tibetan plateau, is the rate of change in melt rate over time, which has been growing exponentially over the past 100 years. Many factors impact the glacial melt rate, but a large part of the problem is caused by debris

Figure 1: The Hindu Kush Himalayan Region (highlighted in green).

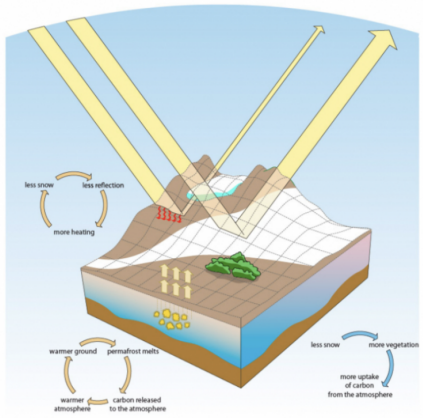

Figure 2: A visualization of the albedo effect on mountain ranges. The darker areas, depicting exposed land, absorb most of the solar radiation while the lighter areas reflect it.

and sediment build-up. Debris-covered glaciers are defined as glaciers with a continuous layer of supraglacial debris over the ablation area, typically increasing in thickness towards the terminus.' These types of glaciers are especially susceptible to the impacts of solar radiation; this is due to the albedo effect (Figure 2). The albedo effect refers to the ability of surfaces to reflect light, with light-coloured surfaces reflecting more light radiation and dark-coloured surfaces absorbing the light radiation.' One can see how the albedo effect factors into the melting of the glaciers as thin debris-covered glaciers see significantly faster rates of melt compared to clean glaciers. A3 /15 pt analysis of this effect on glaciers will be discussed later.

1.1 Tools

Satellite imagery provided by NASA Worldview was utilized to analyze the albedo effect on Earth's surfaces. NASA Worldview is a data archive and visualization system built on NASA's EarthObserving SystemData and Information System. It allows for in-depth visualization of different types of science data sourced from satellite images." The coloration defines the spectrum of albedo strength; deeper hues of red indicate a strong albedo effect, while paler greens indicate a weak albedo. The percentages represent how much light is reflected off of the surface. For example, an albedo value of 0.50 means that the surface reflects 50 percent of the incoming solar energy.

2 Results

The increasing glacial recession rates pose significant dangers to the local environment; however, another primary hazard that the melting glaciers have on the environment is the excess meltwater from the faster rates of melt. With rising regional temperatures of 0.15-0.60C per decade (over the last four decades), the HKH region has seen an increase in the average glacial mass recession rate of about 10-15m/year.'The excess meltwater from the glaciers leads to a drastic increase in water abundance, often creating new and altering existing glacial lakes. While this may seem to be a beneficial outcome for the environment, it is quite the opposite. Increasing temperatures, concomitant with excess meltwater, lead to much higher risks for GLOFs. This is a severe danger to downstream communities as they are openly subjected to devastating destruction. This review article aims to address the dangers of the chronic recession rates of the HKH region's glaciers, provide insight into potential solutions, and shine a light on how global warming is directly affecting humans. The article will also address the socioeconomic concerns regarding the local habitation near large melting glaciers. The review will attempt to verify the inverse correlation between the implications of the albedo effect on the HKH region glaciers, in turn, producing significant amounts of excess meltwater, creating new PDGLs and thus increasing the risk of GLOFs. Rates. Upon inspecting the MERRA-2 Surface Albedo (Monthly) layer on the HKH region, we found that the Albedo effect on Earth from 1980 (the earliest year with available data) to 2020 surface becomes much weaker. Figure 3 shows the surface albedo percentages of the HKH region on February 1, 1980. The left side of Figure 3, for example, shows high albedo for the Karakoram mountain range system of Kashmir, on the western side of HKH near the India-Pakistan border. This range contains the Siachen glacier, one of the world's largest mountain glaciers, also suffering from various anthropogenic effects. Since 1989, the Siachen glacier

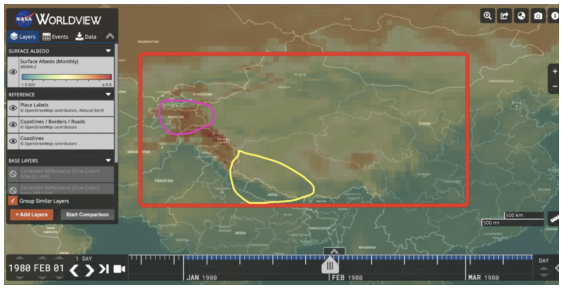

Figure 3: The albedo effect on February 1st, 1980. The red outline shows the general area of the HKH region. The yellow outline shows areas with debris-covered glaciers, such as the Gangapurna and Annapurna III glaciers.

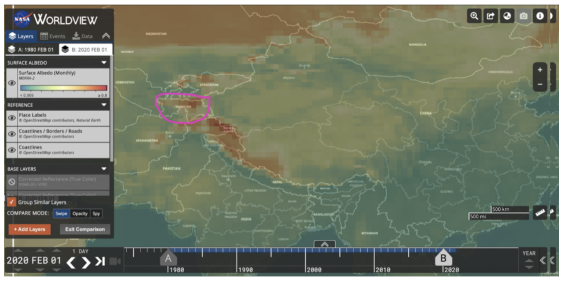

Figure 4: The albedo effect on the HKH region on February 1st, 2020. The Pink outlined area marks the Fedchenko Glacier in 2020.

has been melting at high-speed rates, receding about 2 km in length and experiencing a 17% mass loss.' Today, the Siachen glacier spans 70 km and feeds into the Indus River system, one of the HKH region's ten largest rivers. On February 1, 1980, the albedo percentages of the Siachen glacier averaged around 65%, which is very high for land surfaces, indicating that large volumes of ice and snow were present. On the contrary, in Figure 4, the albedo effect in the same region is much more subtle; the albedo percentages around the same area, on February 1, 2020, average around 57%. This decrease in reflectivity indicates that the effect is much weaker in 2020, compared to the 1980's results, which was expected. This outcome is due to a combination of the Siachen glacier's high melting rates and the increasing amount of sediment build-up around the area. These results suggest a particularly interesting relationship between the albedo effect and the glacier recession: an inverse relationship. Figures 2 and 2.1 show that many of the glaciers in the HKH region are covered with debris as the albedo percentages around the area consistently dropped between 1980 and 2020. This is especially noticeable on the Fedchenko glacier in Pamir, Tajikistan (Figures 2 and 2.1). These results suggest a particularly interesting relationship between the albedo effect and th 3 36 an inverse relationship. Furthermore, revisiting the relationship between debris-covered ice and the albedo effect, figures 2 and 2.1 clearly show that many of the glaciers in the HKH region are covered with debris as the albedo percentages around the area consistently drop between 1980 and 2020. This is especially noticeable on the Fedchenko glacier in Pamir, Tajikistan (Figures 2 and 2.1).

3 Discussion

There is an inverse relationship established between the melt rate and the debris thickness. As presented in the case of Fedchenko glaciers, the melt rate is much slower than other glaciers because the glacier's terminus is fully covered by thick supraglacial debris. From 1978 to 2001, the area change of the Fedchenko glacier was only -2.91 km^2, with a total area of 580 km2. Compared to the smaller glaciers east of the area, which saw an area reduction of almost 20% in the same time period, the Fedchenko glacier is surprisingly stable. even though it has lower albedo levels. Conversely, slower recession rates caused by the debris-cover anomaly do not always produce a positive result. Many debris-covered glaciers are only protected near the glacier's terminus, which means the glacier head is usually exposed to clean ice. This results in a greater mass loss up-glacier compared to its terminus, which causes the glacier to stagnate.' This process is especially dangerous because the water build-up on the terminus of the glacier forms supraglacial lakes (Figure 2.6), while the excess debris build-up helps in the creation of moraine-dammed lakes, or proglacial lakes. Moraine-dammed lakes are also a direct result of the glacial recession. When glaciers recede in length, debris from the terminus gets transported to the front of the glacier, creating a type of sedimentary dam. As a result of the debris build-up, new glacial lakes were created, and GLOFs have been increasing in frequency over the last 100 years. In the last four decades, over 40 GLOFs have occurred in the HKH region.' Many of these disasters resulted in many deaths along with billions of dollars in infrastructure damage. In 2018, Prakash and Nagarajan did a GLOF risk assessment of the Chandra basin (Figure 3), identifying the different PDGLs in the area.' In the Chandra basin, there are 355 glaciers, all of which are melting at increasing rates, which dangerously creates new lakes and expands existing ones. Figure 3 suggests there are many settlements along the Chandra River, making them very vulnerable to

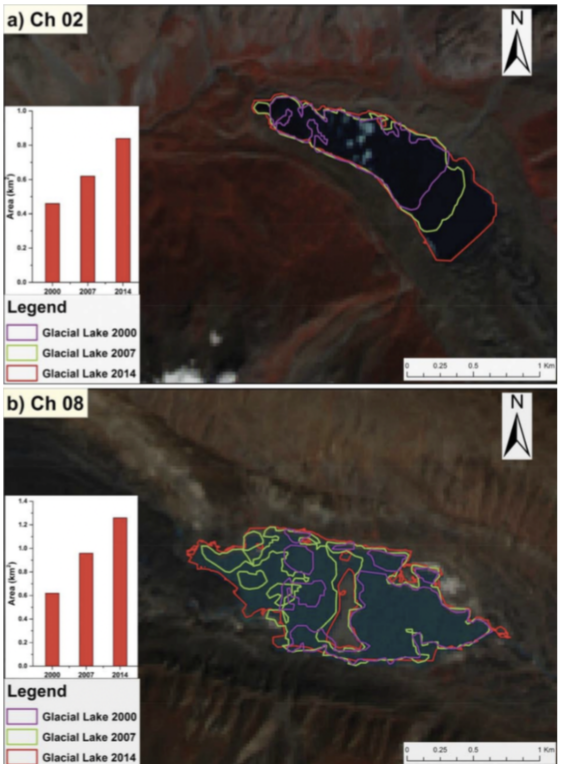

Figure 5: Two glacial lakes determined to be highly susceptible to outbursts. The outlines show these lakes experienced tremendous rates of growth.

GLOFs, and thus these threats must be mitigated. From 2000 to 2014, 18 new glacier-fed lakes appeared in the basin, which resulted in a 64% increase from 28 lakes in 2000 to 46 lakes in 2014. From these 46 lakes, seven of them were identified to be PDGLs, with two moraine-dammed lakes being declared to have high outburst probability, which was expected (Figure 5). Moraine-dammed lakes are the most dangerous as they are very poorly secured. The proglacial debris is comprised of loosely packed sediment, and they often show a low width-to-height ratio with the glacier, making them highly open to outbursts.'6 Along with outburst floods, the degradation of weak moraine dams can also create landslides or ice avalanches, posing an additional greater threat to downstream establishments. Supraglacial lakes are also hazardous as the water build-up on these glaciers drains through the debris and the glacier itself, creating fractures in the ice, which accelerates the ablation rate of the glacier. Consequently, a large outburst flood is created when the water build-up becomes too great for the ice dam. An example of moraine-bordered glaciers that can create landslides and even floods due to the glacial recession is the relatively recent 2013 GLOF in Uttarakhand. A study was done by Allen et al. (2015),2" focusing on the essential factors of this particular incident. On June 17, 2013, heavy precipitation and high temperatures caused the outburst of the Chorabari Lake in Northern Indi, near the Chorabari glacier in Northern India. The Chorabari lake initially formed due to the excess meltwater from the terminus of the Chorabariglacier. From 1962 to 2012, one year before the flood, the Chorabari glacier retreated 344 ± 24 m in length, leaving behind large piles of debris, which dammed in the lake.22 Before the burst, the lake was measured to be around 250m long and 150 m wide, with a water depth of 11 to 15 m, holding around 262 million liters of water, The actual outburst resulted from the heavy precipitation, combined with unusually rapid snow depletion, which eroded its moraine dam, discharging large volumes of water and carrying rocks downstream to the Kedarnath village. The flood claimed over 6000 lives and displaced over 100,000 people from their homes. In addition, roads and hydroelectric power projects were destroyed, leaving millions of dollars in damages. Four weeks before the flood, rapid snowmelt occurred due to the high summer temperatures, flooding the lake with even more water. The lake also lacked a stable outlet channel, which further added to the problem as the water had no way out. The moraine dam was also fragile as it was built on loose rocks and dirt left behind from the Chombari glacial retreat. As a result of these different factors, the disaster could have been foreseen due to the minor signs of outburst that the lake showed; however, no one investigated the issue. In summary, the 2013 Chorabari GLOF proves the positive relationship between the glacial recession and changes in glacial lakes. As the Chorabari glacier retreated and the snow melted, the meltwater flooded into the Chorabari moraine-dammed lake, which eventually outbursts and wreaked havoc on the land. In essence, the positive relationship between the glacial recession rate and the changes in glacial lakes has been verified. In the Chandra basin, the glaciers saw an average rate of retreat of 0.1 to 0.5% per year between 1988 to 2007.' Around the same time, in 2000, the number and area of glacial lakes increased by 64%, proving that glacial meltwater is the leading source of water for lake expansions. This further supports the direct relationship between glacial recession rates and lake changes: as recession rates increase, glacial lakes increase in size and quantity, which additionally endangers downstream communities. It can also be seen that the relationship is inversely related to the albedo effect on glacial recession rates: as the

albedo effect gets weaker on glaciers, more debris is built up, and thus glacial lakes see greater changes, accelerating recession rates. These relationships are crucial to our understanding of how the environment is correlated with itself, allowing us to predict the different outcomes and threats imposed on the HKH region.

4 Conclusion

In conclusion, understanding the correlation between the albedo effect and anthropogenic glacial recession is critical to predicting future glacial lake outbursts. Throughout this review, past glacial recession data and satellite imagery from Google Earth and NASA Worldview were examined to determine the intercorrelation between the three variables: albedo effects, glacial recession, and glacial lake changes. The ChorabariGLOF was a key example of the severe human consequences of neglecting the early signs of glacial lake outburst. More accurate predictive tools such as albedo effect analysis could assist government officials and geologists in monitoring the Chorabariglacial Lake for potential GLOFs. On June 16, 2013, scientists checked the Chorabari lake; however, it was too late as it experienced an outburst the next day. After the destruction, the Uttarakhand government initiated a construction project to build a flood protection wall in 2015, two years after the disaster. Accurate prediction tools could have prevented the destruction of the patterns of the Chorabari Lake changes had been acknowledged. Possible solutions could include the extraction of water from PDGLs, which could be used by the community, or the construction of glacial lake drainage systems. Either of these solutions could have been implemented before the Kedarnath flood, benefiting the township with extra resources, as well as ensuring safety.

References

[1] Wester, P.:; Shrestha, A. B.; Mishr, A.; Mukherji, A. The Hindu Kush Himalaya Assessment: Mountains, Climate Change, Sustainability and People. [2] Ahmad, O. Explainer: The disappearing glaciers of the Himalayas.

[3] Bajracharya, S.; Shrestha,B.The status of glaciers in the Hindu kush-himalayan region.

[4] Ely, J, Debris-covered Glacier Land Systems.

[6] Prakash, C.; Nagarajan, R. Glacial lake changes and outburst flood hazard in Chandra basin, North-Western Indian Himalaya.

[7] Earth Observing System Data and Information System (EOSDIS).

[8] Kumar A, Singh P, Raizada P, Hussain CM. Impact of covid-19 on Greenhouse Gases Emissions: A critical review [Internet]. Science of The Total Environment.

[9] The Editors of Encyclopaedia Siachen Glacier.

[10] Lambrecht, A.; Mayer, C.; Aizen,V.; Floricioiu, D.; Surazakov, A. The evolution of Fedchenko glacier in the Pamir, Tajikistan, during the past eight decades. Journal of Glaciology.

[11] Reznichenko, N.; Davies, T.; Shulmeister, J.; McSaveney, M. Effects of debris on ice-surface melting rates: an experimental study. Journal of Glaciology 2010.

[12] Dong K, Hochman G, Zhang Y, Sun R, Li H, Liao H. emissions, economic and population growth, and renewable energy: Empirical evidence across regions [Internet].

[13] Smith LV, Tarui N, Yamagata T. Assessing the impact of COVID-19 on global fossil fuel consumption and emissions [Internet]. Energy Economics. North-Holland; 2021

[14] Rasul, G.; Dahe, Q.; Chaudhry, Q.Z. Global Warming and Melting Glaciers along Southern Slopes of HKH Ranges.

[15] Evans, S. G. A review of catastrophic drainage of moraine-dammed lakes in British Columbia.

[16] Allen. S.K.; Rastner, P.; Arora, M.; Huggel, C.; Stoffel, M. Lake outburst and debris flow disaster at Kedamath.

[17] Mehta, M.; Dobhal, D. P.;Kesarwani, K.; Pratap, B.; Verma, A.; Kumar,A. Monitoring of Glacier Changes and Response Time in Chorabari Glacier.

[18] Srivastava, S. Glacier burst - a killer disaster; but the solution lies in managing cascading risks.

[19] Dandabathula. G.; Sitiraju, S.R.; Jha, C.S. Investigating the 7th February 2021 landslide triggered flash flood in the Himalayan region using geospatial techniques.

[20] Sakai, A.Glacial Lakes in the Himalayas: A Review on Formation and Expansion Processes.

Linguistic Hurdles Shaping Opportunities in the Immigrant Integration Experience

Siddharth Munjal

January 23, 2024

Abstract

There is a multitude of languages spoken worldwide, yet English has emerged as the predominant one, widely accepted as the international standard. However, not everyone can communicate through this "standard". Even if they can, they may not communicate at the level of proficiency comparable to someone from America or England. Most of the people who are classified as having the ability to speak English are not from either of these regions, thus not indulging in the "standard" that the world keeps as a form of universal communication. The social norm is to speak English with some level of an American accent, resulting in that being the national language spoken without it being declared as the official one by the government. The principle is when speaking with anyone unknown everyone is "assumed" to know at least English. Individuals speak with their variation and accent, which come from the country/region of which they are from. Thus, they will naturally have speech that is distinctly different not only from the "Standard American English", but also from other countries/communities' versions of English. Due to this predicament, there is a challenge for those speaking with different accents and variations to speak with one another, even if everyone is doing so in what they have learned in English.

Keywords

Language, English, Immigrant, Employment

1 Introduction

Lack of coherent communication is an obstacle to the progression of a society. A society requires constant disclosure and connection not only for going about the day but also to produce significant innovation. America would never be the height of economic power it is today with no communication between immigrants. America fundamentally is a world experiment that is made up of immigrants, not legacies of people going back thousands of years like India or China. However, the prospect of everyone speaking a different language within the borders of America could potentially undermine the social cohesion prevalent today. To mitigate such challenges, similar to how English became the default language for international travel, America has adopted English as the default language due to its diverse, international population. One specific challenge faced by immigrants working for companies in foreign countries, or even working remotely for American businesses, is the issue of convertibility upon entering the American workforce. The difficulty in conveying thoughts and ideas is a tangible hurdle that immigrants encounter. Addressing this challenge requires comprehensive language programs and establishing connections with other immigrants who have navigated similar linguistic barriers. In conclusion, the global adoption of English as a connecting language has undoubtedly facilitated communication on an unprecedented scale. However, the nuances, variations, and challenges associated with this linguistic shift highlight the need for a nuanced approach to foster effective communication, social cohesion, and the continued success of societies built on the diversity of languages and cultures.

2 The American Atmosphere Surrounding Meritocracy

Immigrants coming to America thus have to deal with the companies/businesses that are foreign to them in terms of culture and structure. For the foreseeable future, this will always be a circumstance

with "nearly three-fourths (72%) of Americans believe immigrants come to the United States to "find jobs and improve their lives" (Ekins & Kemp, 2021). The main objective of a business is to make a profit. Amongst a free market, capitalism leads to lower prices, higher quality, and increased economic prosperity through the competition of businesses meddling in products and services. The best way to succeed in a business is to cater to the needs of your customers. Thus, making a business oriented for ease by customers is crucial, where the reputation and overall growth are on the line. However, that does lead to those coming from or working from overseas to find employment, especially for those speaking accents foreign to America in this case. For example, immigrants who travel to America will have to speak with people here. There is a high enough probability that those here will have a "standard American" accent compared to the immigrants coming over here. The immigrant will then more likely be facing difficulty in their daily life due to not of the native culture and language, even if they speak some variation of English already. For example, language barriers "lead to a lack of confidence, inhibiting many from speaking up and participating in class, and ultimately missed job and educational opportunities" (Roshi, 2018). As such, there will be an inevitable push for immigrants to make themselves of the place they have moved in the culture and ways of life. Due to less feasible communication between natives and immigrants, a business will then be incentivized not to put them in the position of customer service due to the difficulty they might have conversing with the customer. Thus, causing the business to have less ease for the customer to obtain a product/service or assistance. A business will optimize the resources to grow to its highest capacity, which means it does not handle inconsistencies well. The immigrant will more than likely be put to work in other roles such as IT or accounting, where they are more of an expert and can contribute the most. By this, businesses can be termed "linguistically" harmful. Another way is by the professional degrees of different educational institutions not deemed as capable as those of in the West compared to poorer countries. Even if the technical knowledge is the same, there is no standard test or transition provided to test their capacity to work in the American marketplace. A doctor, for example, may know the knowledge and have the capacity to the highest ability, but due to the language barrier, the immigrant doctor has a harder time fighting for their case. Thus most of the time, if they wish to work in America, they are forced to go back to medical school again. However, regardless of any part of the life of an immigrant in a new country, they will have trouble going about life due to such changes, forcing them to adapt.

3 Proposition

3.1 Problem with Linguistic Divide

Speech is not something that can remotely be made "equitable" as liberals like to term it. If you have fewer skills (such as the capacity to speak in a certain manner), then you will fall short naturally to some degree and become restricted. However, regulating businesses based on "speech discrimination" by implementing policies such as quotas to accommodate migrants is a very dangerous precedent. Attempting to make a skill or ability of an individual equalized on the playing field not only leads to less incentive for individuals to progress through merit but can also push other "equalizing regulations" that can lead to speech restrictions. Regulations on a very unenforceable offense are not practical and can easily become abusive. This is different than prosecuting a business for discriminating based on race/ethnicity, where just by the look of the individual is then given a certain task or designated a role instead of based on skill and merit. In this way, "linguistic discrimination" as termed by liberals, is not very practical to push against from the position of a government role.

3.2 Solution

One way to solve the issue of an individual, such as an immigrant, not having the capacity to speak in a certain manner based on accent and linguistic ability is through enforcing programs within businesses for said individual. The individual naturally would be inclined to do such a course because not only would it help develop their skills for progressing in a business environment, but also within all aspects of daily life in a new country (such as America). Lack of linguistic ability makes all portions of life difficult, both personally and professionally. The eventual goal would be for the individual to learn English to the point that not only can said individual converse with others for mutual understanding but also to have them grow in their position of the institution or business they attend or work for,

respectively. Thus, learning English through such programs would be very beneficial and would assist the country overall with more capable productive members of society. Another solution is having them connect with others from similar backgrounds such as through ethnicity or country of origin. As such, "Maintaining a support structure with others, particularly those going through the same experience" can help with the transition to a new place (US Department of State). Individuals of similar backgrounds are much more likely to make connections with each other easier because not only do each other understand the experiences of the other, but they also are much more comfortable psychologically with another person who resembles them. In this, individuals can help each other navigate the place that they have now called home not only within businesses but also in daily life. They can act as the bridge for each other about the place they just left behind while also adapting to the new way of life.

4 Conclusion

Overall, this issue does have validity due to such a transition from one place to another is difficult, and having to figure out the customs and language of a new place while making an earning on top. However, such situations do pan out, especially when immigrants come with the mindset of working hard in all portions of life. For this reason, immigrants on average are richer and pay higher taxes than native-born Americans. The average annual salary nationwide for Americans is $59,428 (Wong, 2023). In comparison, the average annual salary nationwide of an immigrant in America is $90,223 (ZipRecruiter, 2023). Nonetheless, there is always room for improvements to assist in the progression of individuals overall, especially those attempting to grow and expand their roots in a completely new country. Two of the proposed solutions for helping linguistically through such a transition within the business of another country are English language courses and connections to others. These both will help to build the bridge for immigrants to not only improve on skills (which will help in a business) but also throughout their lives going forward overall. Regulations of linguistics on a large scale are not practical, but what is practical are social practices that can be done within communities and groups to hold up individuals (in this case immigrants). Immigrants are what make up America, and each individual (whether classified into a group or not) will have to adapt and change to succeed in a new society just as they would moving to another country. However, the reason immigrants are driven is due to the lack of opportunity and high poverty that they experienced in their home countries. Therefore, when given the chance to go to a new place that gives the chance for social mobility, they accept the principle and work towards pushing themselves.

References

[1] Belle Wong, J.D. "Average Salary by State in 2023." Forbes, Forbes Magazine, 8 Nov. 2023, www.forbes.com/advisor/business/average-salary-by-state/. Accessed 9 Dec. 2023.

[2] Ekins, Emily, and David Kemp. "Poll: 72% of Americans Say Immigrants Come to the United States for Jobs and to Improve Their Lives." Cato.Org, Cato Institute, 21 Apr. 2021, www.cato.org/blog/poll-72-americans-say-immigrants-come-us-jobs-improve-their-lives53-say-ability-immigrate.. Accessed 9 Dec. 2023.

[3] Roshi, Irfaan. "Language Integration Barriers: Perspectives from Refugee Youth." BRYCS, brycs.org/migration-resettlement-awareness/language-integration-barriers-perspectives-from-refugee-youth/. Accessed 13 Dec. 2023.